Consecutive Reaction Mechanism for the Formation of Spore Photoproduct in DNA Photolesion

Qian Du,[†] Hongmei Zhao,[†] Di Song, Kunhui Liu, and Hongmei Su*

Beijing National Laboratory for Molecular Sciences (BNLMS), State Key Laboratory of Molecular Reaction Dynamics, Institute of Chemistry, Chinese Academy of Sciences, Beijing 100190, China

ABSTRACT: We have explored the potential energy profiles of TpT dinucleotides toward formation of a DNA photolesion product, spore photoproduct (SP), along the S_0, S_1, and T_1 states, by means of density functional theory and time-dependent density functional theory. Together with the spin density analysis, the consecutive mechanism for the SP formation can be established. The detailed reaction pathways have been revealed. All the adiabatic reaction pathways proceeding though S_1, T_1, or S_0 alone are shown to be energetically infeasible, while the nonadiabatic pathway involving both the T_1 and S_0 states corresponds to the lowest-energy path and is the most favorable in energy. The nonadiabatic pathway is rate-limited by the step of the hydrogen atom transfer proceeding in the T_1 state with a barrier of 14.2 kcal mol^{-1} (11.9 kcal mol^{-1} in bulk solution), whereas the subsequent $C5-CH_2$ bond formation toward the final SP formation occurs readily in S_0 after intersystem crossing from T_1 to S_0 via the singlet−triplet interaction. The

results provide a rationale for the experimentally observed kinetic isotope effect after deuterium substitution at the 3′-T methyl group of TpT.
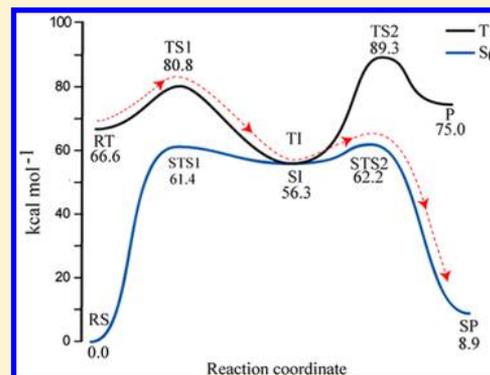
1. INTRODUCTION

Ultraviolet (UV) light is one of the most lethal and potent challenges to living organisms in the natural world. It usually results in DNA photolesion in the cellular systems of organisms and subsequently leads to mutation or even death.[1] In contrast to normal DNA, the bacterial spores, *Bacillus* for instance, express unexpected resistance to UV light, which is due to the formation of spore photoproduct (SP) and a corresponding efficient chemical repair mechanism associated with the catalysis of a specific enzyme, spore photoproduct lysae (SPL).[2] The commonly called spore photoproduct (SP) refers to the special UV-induced pyrimidine dimer, 5-thyminyl-5,6-dihydrothymine, which is formed by linking the allylic carbon to the C5 of the adjacent thymidine (Scheme 1).[3] Upon UV irradiation in the thymidine pair, the spore photoproduct can

be easily formed and maintained in the phase of SP-dimer for a long time, like dormancy. As a result, it prevents spore DNA from further photolesion and other chemical reaction until the specific enzyme (SPL) performs a reversed progress of SP-dimer formation, which enables the recovery of a normal life cycle.[3−6]

Although SP was discovered nearly half a century ago,[7] and despite the strong interest of the scientific community in how it is formed,[3,8] the formation mechanism of SP after UV irradiation is still not completely understood. Two mechanisms have been proposed previously to explain SP formation. Cadet and co-workers[9] raised a concerted mechanism which involves the cross-link of the methyl group of one thymidine and the C═C double bond of the second thymidine (Scheme 2, path A). By irradiating the free base of [D3]thymidine containing a CD3 moiety, they isolated the SP product as a mixture of the 5S and 5R diastereomers after the photoreaction.

Varghese and Wang[10,11] suggested a consecutive mechanism in which the recombination of a 5-α-thyminyl radical and a 5,6-dihydrothymin-5-yl radical leads to the formation of SP (Scheme 2, path B). Very recently, Lin and Li[12] prepared two deuterium-labeled dinucleotide thymine dinucleoside monophosphate (TpT), [D3]TpT, and [D4]TpT and monitored the hydrogen/deuterium atom transfer after UV irradiation by ^{1}H NMR spectroscopy. Their results showed that a hydrogen atom from the methyl group of 3′-T is

Scheme 1. Formation of Spore Photoproduct upon UV irradiation of DNA (Demonstrated with the Dinucleotide TpT)[a]
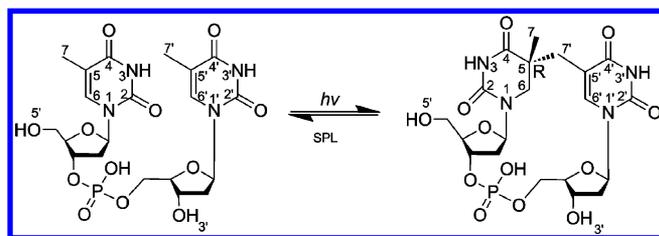
[a]The atomic numbering used hereafter is also labeled.

Scheme 2. Two Proposed Mechanisms for SP Formation: Path A, Concerted Mechanism; Path B, Consecutive Mechanism
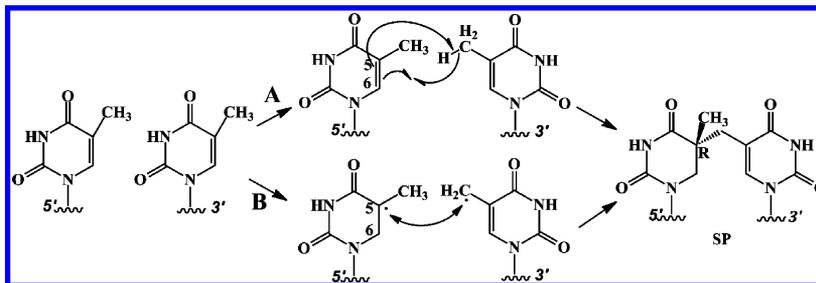
transferred intramolecularly to the C6 atom of 5′-T in a highly diastereoselective manner, from which a more detailed consecutive mechanism was proposed (Scheme 2, path B). It was suggested[12] that the C5=C6 bond of 5′-T was excited by UV light to form biradical triplet excited state. Then one of the hydrogen atoms of 3′-T methyl transfers to the C6 atom of 5′-T, forming two radicals, the 5-α-thyminyl radical and the 5,6-dihydrothymin-5-yl radical, which recombine to the final product SP. But they also pointed out that the concerted mechanism cannot be ruled out. In addition, the proposed radical intermediates had not been observed directly in the experiment. Obviously, further studies are required to confirm the proposed consecutive mechanism.

During the formation of SP, a chiral center is generated at carbon C5, which thus can adopt either an R or S configuration provided that the thymine residues react freely.[3] However, due to the constraints imposed by the double-helical DNA structure, only one of two stereoisomers, 5R or 5S, is possible for SP formed from adjacent thymines in the bacterial spores.[13] It has been established clearly that SP adopts solely a 5R configuration in the photoreaction of natural DNA, owing greatly to the extensive NMR studies[8,12] and crystal structural analysis[14,15] as well as enzymatic-repair studies.[15,16]

The present work mainly focuses on elucidating the photochemical reaction mechanism of SP formation by theoretical means. We choose to calculate the photoreaction of the dinucleotide TpT, which is also the starting reactant employed in most photoreaction experiments, as it is the smallest DNA fragment to accommodate a SP dimer and sustains the constraints of the DNA backbone. The potential energy profiles for the SP formation in the possible lowest-lying triplet and singlet ground state as well as the interaction between these two states are explored at the B3LYP/6-311+ +G(d, p)//B3LYP/6-311G(d, p) level of theory. The reaction pathways on the singlet excited state S_1 are also explored on the basis of TD-DFT calculations using the S_0 stationary structures. The experimentally undetected radical intermediates are allowed to be characterized theoretically by spin density analysis. Together with the energy profile information, the consecutive mechanism for the SP formation can be established and shown to follow a nonadiabatic pathway involving both the T_1 and S_0 states. Moreover, the possibility for a concerted mechanism has been explored and found to lead to a totally different product other than SP, thus excluding its involvement in the SP reaction.

2. COMPUTATIONAL METHODS

In the present work, we choose the smallest DNA fragment, the dinucleotide thymine dinucleoside monophosphate (TpT), as the reaction system. Although it is desirable to use simplified models of two free thymine bases for the sake of computational

efficiency, as reported for dealing with the cyclobutane pyrimidine dimer (CPD) and the (6−4) pyrimidine−pyrimidone photoproduct (TT64) reaction,[17,18] the influence of the DNA backbones (e.g., strain effects) has to be neglected in that case. In the current system of TpT, the relative position of two thymine residues is restricted. The glycoside and the phosphoester will definitely affect the motion and transformation of the pyrimidine residues, despite the fact that the absorption of UV light by DNA results in localization of energy mainly at the sites of the bases. Our reaction system is the same as those used in NMR experiments[8,12,14] and is close to the natural situation of DNA strand, in which the SP reaction takes place between two intrastrand adjacent thymines.

The SP photoreaction is invoked by an initial excitation of thymine residues to a singlet excited state $^1(\pi,\pi)^*$. Aside from returning to the ground state by internal conversion, intersystem crossing (ISC) leads to a long-lived triplet state $^3(\pi,\pi)^*$.[19,20] Despite its low quantum yield, the long-lived triplet state is believed to be quite reactive toward DNA photolesions.

We have calculated the potential energy profiles along the S_0, T_1, and S_1 states for the possible reaction pathways toward the SP formation with the Gaussian 03 program package.[21] The geometries of the reactants, products, intermediates, and transition states along the T_1 or S_0 state were optimized using hybrid density functional theory (B3LYP) with the standard basis sets of 6-311G(d,p),[22,23] which is an appropriate quantum chemical method for the current large reaction system of TpT. The single-point energies were calculated at the B3LYP/6-311++G(d,p) level with the B3LYP/6-311G(d,p) optimized geometries. The harmonic frequency analysis was performed to identify the stationary point as either local minima (reactant, products, and intermediates) or first-order saddle points (transition states). The intrinsic reaction coordinate calculations have been performed to check the connections of the transition states between two local minima.[23,24] Bulk solvation effects were considered by using the integral electron formalism of the polarized continuum model (IEF-PCM).[25]

In parallel, the reaction pathways were also explored on the singlet excited state S_1 on the basis of TD-DFT calculations[26] using the S_0 stationary structures. This implementation computes vertical excitation energies only. In principle, this prevents the exact localization of stationary points on an excited-state potential energy surface. However, within the framework of the van der Lugt and Oosterhoff model[27] in which the geometrical features of the excited-state path are similar to those of the ground-state path, an approximate excited-state potential energy surface can be calculated using ground-state geometries.
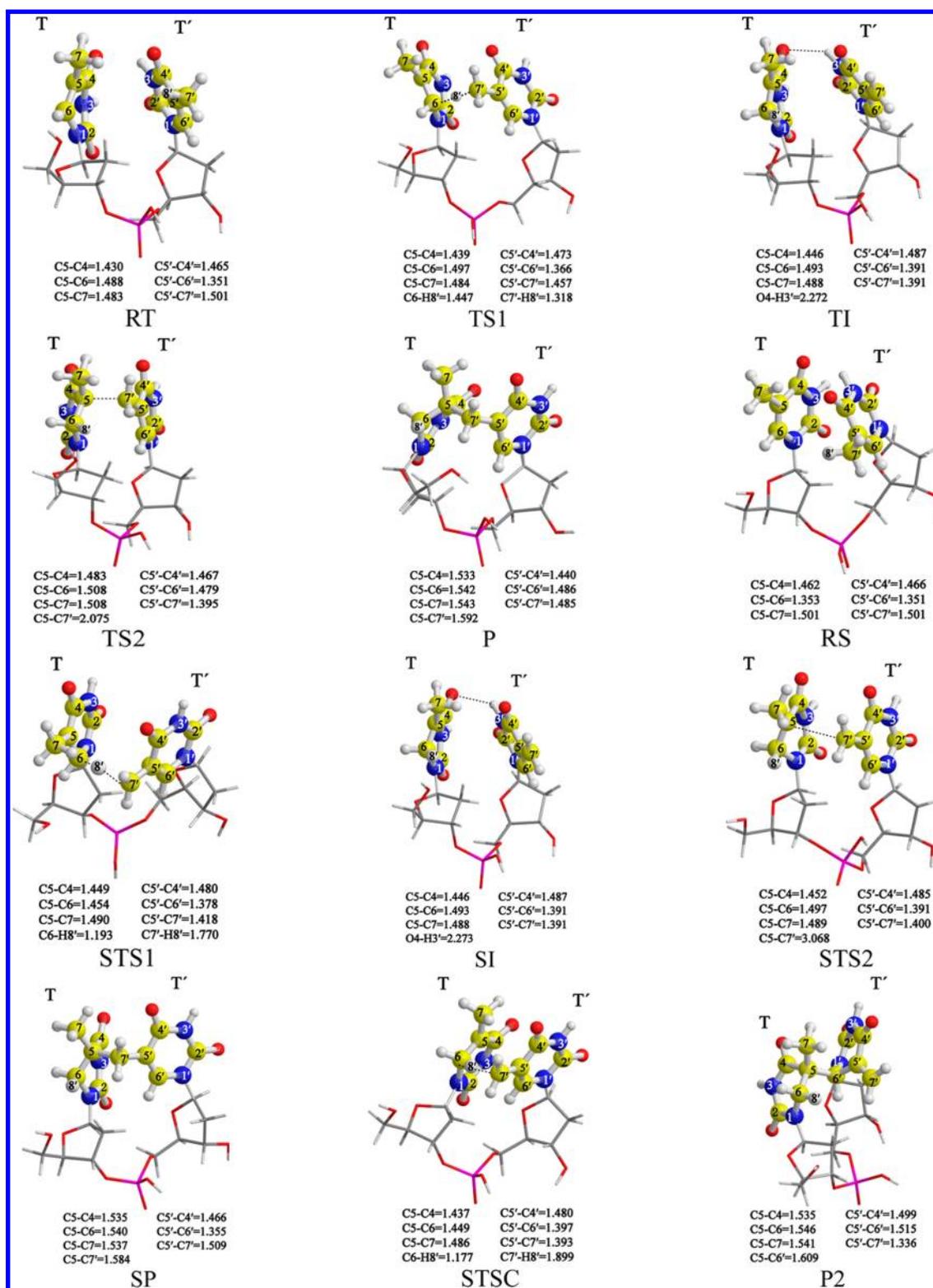
Figure 1. Optimized geometries of reactants, intermediates, transition states, and products in the S_0 and T_1 states at the B3LYP/6-31G(d, p) level. Bond lengths are in angstroms. Carbon, nitrogen, oxygen, and hydrogen atoms are denoted with yellow, blue, red, and gray balls respectively.

3. RESULTS AND DISCUSSION

As shown in Scheme 1, the SP product could result from bond formation between the methyl group of the 3′-end thymine and the C5 atom of the 5′-end thymine residues (5′ → 3′) or vice versa (3′ → 5′). The latter case (3′ → 5′) usually occurs in chemically synthesized spore photoproduct analogues lacking a

DNA backbone. However in the former case, the reactions forming the 5′ → 3′ spore photoproduct have been shown to be favored in natural DNA with conformation constraints, because much shorter distances exist between the C5 atom of the 5′-end thymine and the methyl of the 3′-end thymine moiety (for conformation A of DNA: C−C distance between

the Me$_{3'\text{-end}}$ and C5$_{5'\text{-end}}$ is 3.69 Å and between Me$_{5'\text{-end}}$ and C5$_{3'\text{-end}}$ is 5.52 Å).[8] Therefore, we focus our calculations on the 5′ → 3′ SP reactions, which represent the realistic case in natural DNA.

The potential energy profiles along the S$_0$ and T$_1$ states were calculated with the DFT method, and the reaction pathways on the singlet excited state S$_1$ were also explored on the basis of TD-DFT calculations using the S$_0$ stationary structures. The optimized steric structures of reactants, intermediates, transition states, and products are shown in Figure 1. The computed single-point energies are listed in Table 1. The

Table 1. Relative Energies (without ZPE Correction), in kcal mol^{-1}, of the Stationary Structures along the T$_1$ and S$_0$ Reaction Pathways

	B3LYP/6-31G(d,p)		B3LYP/6-311++G(d,p)	
	vacuum	$\varepsilon = 4.3$	vacuum	$\varepsilon = 4.3$
RS	0.0	0.0	0.0	0.0
RT	66.5	66.8	66.6	66.9
TS1	82.7	81.2	80.8	78.8
TI	57.0	57.1	56.3	56.5
TS2	90.4	89.2	89.3	87.9
P	73.4	74.5	75.0	76.0
STS1	63.6	61.8	61.4	59.0
SI	57.0	57.2	56.3	56.5
STS2	64.3	62.7	62.2	60.3
SP	8.6	7.8	8.9	8.0
STSC	71.6	71.5	70.4	70.1
P2	32.4	32.3	31.4	31.2

potential energy profiles are presented in Figure 2 and Figure 3. The effects of including zero-point energy (ZPE) corrections little affect the reaction barriers and thus in the following are not taken into account.

For the ground-state TpT, two thymine bases (denoted as T and T′, respectively) adopt face-to-face configuration, as shown in RS of Figure 1. A consecutive reaction pathway is revealed, as seen in Figure 2a. In the reactant RS, the C5−C6 bond (1.353 Å) and C5′−C6′ bond (1.351 Å) of the two bases possess the ethylenic double-bond character. Hydrogen atom H8′ migrates from the methyl C7′ in T′ base to C6 in T base via STS1, leading to the formation of the intermediate SI. In the transition state STS1, the C6−H8′ distance is 1.193 Å and the C7′−H8′ distance is 1.770 Å. This step faces a barrier height of 61.4 kcal mol^{-1}. The formed intermediate SI lies 56.3 kcal mol^{-1} above the reactant. Such an unstable species corresponds to the previously proposed radical intermediates, 5-α-thyminyl and 5,6-dihydrothymin-5-yl (Scheme 2), which are bonded to each other by the phosphate and the deoxyribose groups. The intermediate SI is thus of a biradical character. In the intermediate SI, the bond length of C5−C6 has been stretched from 1.353 to 1.493 Å, indicating its conversion to the single-bond character due to the hydrogen atom addition.

After the formation of SI, the cross-link of the allylic C7′ carbon to the C5 atom of the adjacent thymidine (C5−CH$_2$ bond formation) occurs, leading to the final SP product, with a quite low barrier of 5.9 kcal mol^{-1} via the transition state STS2. In STS2, the C5−C7′ distance is 3.068 Å, and the C5−C6 bond, C5−C7 bond, and C5−C4 bond are 1.497, 1.489, and 1.452 Å, respectively.

Bulk solvation with the dielectric constant $\varepsilon = 4.3$ is used to simulate the apolar surroundings in DNA.[28] As shown in Table
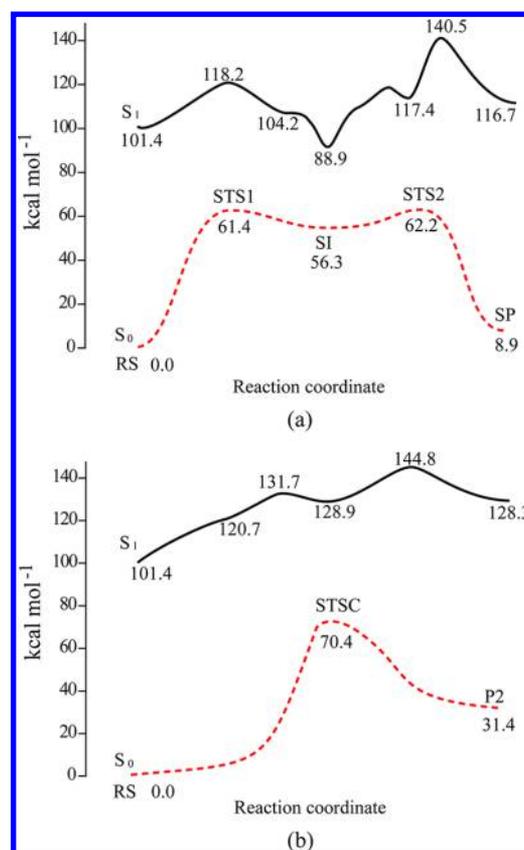
Figure 2. Potential energy profiles on the S$_0$ and S$_1$ surfaces: (a) consecutive reaction pathways toward SP formation; (b) concerted reaction pathways toward the C5−C6′ cross-linked product P2. The relative energies are indicated in kcal mol^{-1}.
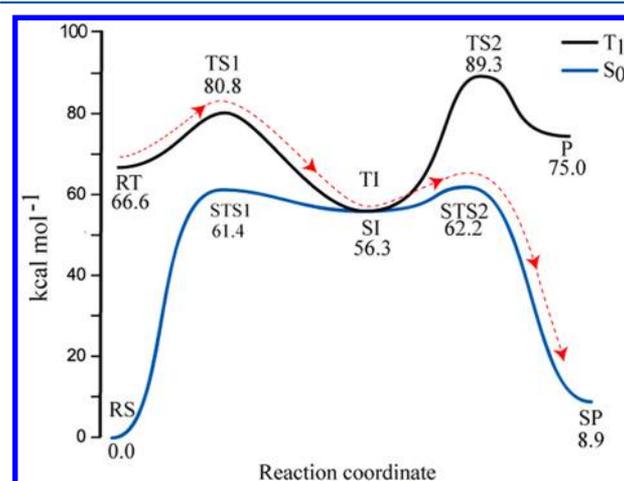
Figure 3. Potential energy profiles of the reaction pathways along the S$_0$ and T$_1$ surfaces. The relative energies are indicated in kcal mol^{-1}. The red dotted line highlights the nonadiabatic reaction pathway.

1, the bulk effects only slightly influence the stationary point energy and the barrier height. The transition-state energies of STS1 and STS2 are lowered to 59.0 and 60.3 kcal mol^{-1}, respectively, compared to the corresponding gas-phase values of 61.4 and 62.2 kcal mol^{-1}. The whole reaction process in the singlet ground state exhibits high barriers. The thermally-driven formation of SP in the ground state is thus energetically inaccessible.

For the photochemical singlet reaction pathway along the S_1 state, the approximate potential energy profile is obtained by TD-DFT calculations and shown in Figure 2a. It reveals an energy barrier of 16.8 kcal mol^{-1} before the system reaches a potential well. Calculated with a nuclear configuration of the S_0 biradical intermediate (SI), this local minimum is 32.6 kcal mol^{-1} vertically above SI. Such a large energy gap indicates a low possibility for radiationless transition from S_1 to S_0. Moreover, the subsequent transformation from the potential well to the final product has to overcome a 51.6 kcal mol^{-1} barrier (transition state at 140.5 kcal mol^{-1}), which is energetically inaccessible. Therefore, the direct SP reaction on the S_1 potential surface is infeasible.

For the photochemical triplet reaction pathway along the T_1 state, the obtained potential energy profile is displayed in Figure 3. Originated from the C=C $\pi \rightarrow \pi^*$ excitation, the main structural feature of the lowest-lying triplet state of the dinucleotide TpT (denoted as RT) is the transformation of the C5–C6 π-bond (1.353 Å) into a σ-bond (1.488 Å) in one thymine base, while the other thymine residue remains intact (see the structure in Figure 1). Correspondingly, the triplet TpT can be envisioned as a biradical species with spin densities mainly localized on the ethylenic C5 and C6 atoms. Thus, the C5 and C6 atoms become reactive and can invoke the cross-link of the two thymine residues forming SP dimer. The reaction pathway along the triplet state is also found to proceed consecutively as shown in Figure 3.

The first step is the H8′ migration from the methyl C7′ of T′ to C6 of T via TS1, which proceeds facilely with a low barrier of 14.2 kcal mol^{-1}. In the transition state TS1, C6–H8′ distance is 1.447 Å and C7′–H8′ distance is 1.318 Å. Taking into account the bulk solvation effect, this barrier is reduced to 11.9 kcal mol^{-1}. The intermediate TI lies 10.3 kcal mol^{-1} below the triplet reactant RT, indicating that the hydrogen migration is an exothermic process. In the intermediate TI, a p–π conjugation occurs for the T′ base among the allylic C7′ carbon and the ethylenic C5′ and C6′ carbons as indicated from the shortened C5′–C7′ bond (1.391 Å) and elongated C5′–C6′ bond (1.391 Å) compared to those in RT, that is, C5′–C7′ bond (1.501 Å) and C5′–C6′ bond (1.351 Å). Thus, the triplet radical intermediate TI is more stable relative to the reactant RT. Bulk solvation affects slightly the exothermicity (10.4 kcal mol^{-1}). Considering the exothermicity and low barrier, it is expected that the hydrogen atom transfer from the T′ thymidine to the T thymidine can take place favorably on the triplet surface.

However, the consecutive step from TI to TS2, which is the cross-link of the allylic C7′ carbon to the C5 atom of the adjacent thymidine, requires surmounting a high energy barrier of 33.0 kcal mol^{-1}. Moreover, the resulting triplet SP photoproduct (denoted as P) is quite unstable, which lies 75.0 kcal mol^{-1} above the initial reactant RS. Thus, there is little possibility that the SP formation occurs solely on the triplet surface. Possibly, surface interactions may exist between the lowest-lying triplet and the singlet ground state, which is crucial for understanding the SP formation mechanism.

For the singlet diradical SI, the two unpaired electrons are distributed to different sets of atoms C5 and C7′. The distance between C5 and C7′ is 5.513 Å. It is obvious that the two singly occupied molecular orbitals (SOMOs) of SI are localized on the C5 and C7′ and shows a typical disjoint character. The Coulombic repulsion energy arising from electrons of opposite spin is minimized. As a result, the biradical species in its singlet

and triplet state are nearly degenerate in principle.[29,30] Indeed, as shown in the calculated potential energy profiles of Figure 3, the singlet biradical SI is equal to the triplet biradical TI in energy, from which the singlet–triplet surface intersection results. To obtain the singlet–triplet interaction profile, the PES was scanned from TS1 to TI by varying the C7′–H8′ distance from a configuration which is close to the TS1 (the initial optimized value is 1.76 Å in that structure) with a step length of 0.6 Å and optimizing the remaining coordinates. The energy scans for the singlet and triplet (both in vacuum and in solution) are displayed in Figure 4. It is noticed that the energy
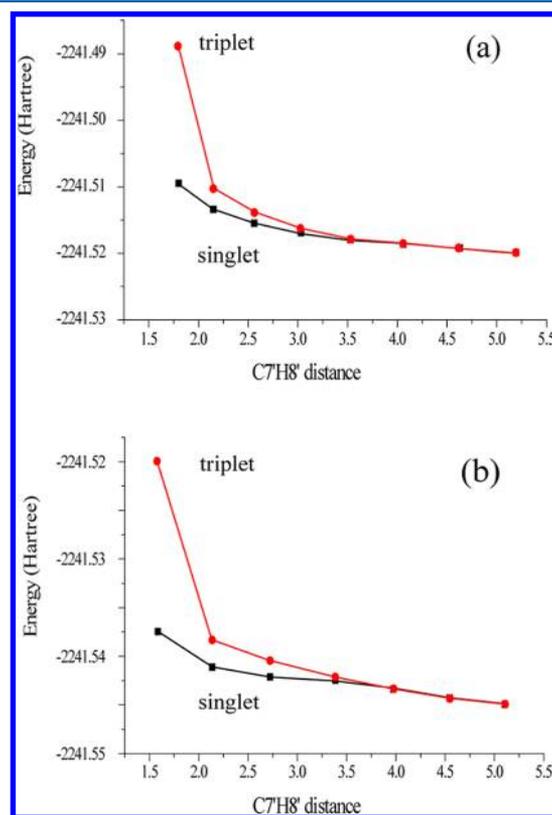
Figure 4. Relaxed potential energy curves for the ground singlet and triplet states, obtained at the level of B3LYP/6-311G(d, p): (a) in vacuum; (b) in solution.

curves get closer and closer when approaching TI and finally equalizes with each other, both in vacuum or in bulk solution, proving further the triplet–singlet surface crossing.

The T_1/S_0 surface crossing located at the biradical intermediates (TI and SI) can facilitate the reaction process substantially. The first step of hydrogen atom transfer proceeds easily in the triplet PES with a low barrier of 14.2 kcal mol^{-1} (11.9 kcal mol^{-1} in bulk solution), leading to the intermediate TI. It is hard for TI to pursue the subsequent C7′ linking to C5, with a high barrier of 33.0 kcal mol^{-1}, on the triplet surface. Instead, the triplet intermediate TI tends to cross over to the singlet state SI because of the T_1/S_0 surface crossing, and complete the C7′ linking to C5 thereafter, which is quite facile in the ground state because it has a barrier of only 5.9 kcal mol^{-1} (reduced to 3.8 kcal mol^{-1} in bulk solution). This energy barrier is drastically lower than that in the triplet surface from TI to TS2. Therefore, the SP formation reaction should follow such a consecutive mechanism including the T_1 state hydrogen atom transfer and the S_0 state cross-link of allylic C7′ to C5, as

highlighted with the red dotted lines in Figure 3. This is a nonadiabatic pathway involving the participation of both the T_1 and S_0 states. Compared with the other adiabatic reaction pathways proceeding through S_0, S_1, or T_1 states alone, the nonadiabatic pathway is rate-limited by a much lower barrier of 14.2 kcal mol^{-1} (the step of the hydrogen atom transfer in T_1, which is further reduced to 11.9 kcal mol^{-1} in bulk solution) and thus corresponds to the lowest-energy path. Moreover, the downward potential energy profile exhibited with the nonadiabatic pathway also makes it the energetically most favorable mechanism accounting for the SP formation.

To further establish the consecutive mechanism, the key radical intermediates proposed by earlier experimental work[10,12] are characterized by analyzing spin densities. The spin densities of selected atoms in reactants, intermediates, and products along the most favorable nonadiabatic pathway are listed in Table 2. Following the UV excitation and intersystem

Table 2. Mulliken Spin Densities (e^{-}; B3LYP/6-311+ +G(d,p) Level) of Selected Atoms in Each Species along the Nonadiabatic Reaction Pathway

	C_5	C_6	C_7	$C_{5'}$	$C_{6'}$	$C_{7'}$
RT	0.76	0.70	−0.01	0.00	0.00	0.00
TS1	0.77	0.35	−0.05	−0.12	0.22	0.42
TI	0.81	−0.11	−0.05	−0.21	0.46	0.75
SI	0.81	−0.11	−0.05	0.25	−0.45	−0.75
STS2	0.86	−0.19	−0.05	0.21	−0.40	−0.74
SP	0.00	0.00	0.00	0.00	0.00	0.00

crossing, the triplet excited state TpT is formed (denoted as RT). In RT, the spin density on C5 and C6 is 0.76 and 0.70, respectively, indicating the localization of the unpaired electron densities on the ethylenic C5 and C6 atoms. This confirms the biradical feature of the triplet excited state TpT. The subsequent hydrogen atom abstraction by C6 from the T′ methyl leads to the intermediate TI, where the unpaired electron densities on the C6 atom decrease from 0.70 to −0.11 and those on the C7′ atoms increase from 0.00 to 0.75. Thus, one unpaired electron is transferred from the C6 to the C7′ atom when RT transforms to TI. In this process, the other unpaired electron is still located at the ethylenic C5 atom, as indicated by its spin density of 0.81. But the two unpaired electrons located at the C7′ atom (0.75) and C5 atom (0.81) of TI possess the same spin directions, which hinders the cross-link of the allylic C7′ with C5 in TI toward the final SP formation, although TI is also of a biradical character. This explains why the triplet intermediate TI faces such a high energy barrier of 33.0 kcal mol^{-1} to complete the cross-link and form SP product in the T_1 state (Figure 3).

However, due to the surface crossing, the triplet biradical intermediate TI is apt to cross over to the singlet biradical intermediate SI, where the unpaired electrons are located on C5 (0.81) and C7′ (−0.75) atoms with reversed spin directions, as shown in Table 2. As a result, there is a positive trend to form a σ-bond between C5 and C7′ atoms of the singlet biradical intermediate SI. Naturally, the cross-link of the allylic C7′ with C5 in SI toward the final SP formation is quite facile, as manifested by its low barrier of 5.9 kcal mol^{-1} (3.8 kcal mol^{-1} in bulk solution) in the S_0 potential energy profiles.

From the above analysis of spin densities, the biradical character can be revealed for the intermediates (TI and SI) involved along the consecutive reaction pathways. Although

these biradical intermediates have not been trapped and detected in the experiments, our calculated results confirm their key participation and thus support the hypothesis of the previously proposed consecutive mechanism.[12] Moreover, the necessity for the intersystem crossing of triplet TI to singlet SI (i.e., nonadiabatic pathway) in facilitating the SP formation can be further justified from the spin directions of unpaired electrons.

Our calculation results can provide rationale for previous experimental observations. In the ^{1}H NMR experiments monitoring the hydrogen/deuterium atom transfer after UV irradiation of two deuterium-labeled TpT dinucleotides, [D$_3$]TpT and [D$_4$]TpT, faster photoreaction was observed for the [D$_4$]TpT with all four hydrogen atoms in 5′-T replaced with deuterium atoms, compared with the reaction rate for the [D$_3$]TpT which contains a [D$_3$]methyl group in the 3′-T residue.[12] Their results suggested the existence of a primary kinetic isotope effect (KIE). Furthermore, a primary KIE of 3.5 for the photochemical SP formation was obtained. The observed primary isotope effect of 3.5 after deuterium substitution at the 3′-T methyl group indicated that the hydrogen atom transfer from the 3′-T methyl group to the C6 of the 5′-T residue is potentially rate-limiting.[12] This postulation can be fully supported by our calculations, which show that the most energetically favorable pathway, as highlighted with red dotted lines in Figure 3, is truly rate-limited by the step of the hydrogen atom transfer proceeding in the T_1 state with a barrier of 14.2 kcal mol^{-1} (11.9 kcal mol^{-1} in bulk solution), whereas the subsequent allylic C7′ linking to C5 toward the final SP formation occurs readily in the S_0 state after intersystem crossing from the triplet biradical TI to the singlet biradical SI, with a barrier of only 5.9 kcal mol^{-1} (3.8 kcal mol^{-1} in bulk solution). Vice versa, the experimentally observed kinetic isotope effect supports our conclusion that the nonadiabatic reaction pathway involving both the T_1 and S_0 states is the most feasible mechanism, because if the reaction proceeds in the triplet surface alone, the rate-limiting step is not the hydrogen migration but the allylic C7′ linking to C5, which has a higher barrier of 33.0 kcal mol^{-1}.

Additionally, this mechanism coincides with the observed 5R steric configuration of the SP molecule. In the initial ground-state reactant TpT (denoted as RS in Figure 1), two adjacent thymine bases stand face-to-face and both adopt an anti configuration relative to the deoxyribose moiety. This is the same as the case in spore or dry-state DNA, where an A-like conformation is adopted and the thymine bases are in the anti glycosidic bond conformation domain. As shown in Scheme 1, the anti TpT conformation is anticipated to lead to the SP product with a 5R steric configuration, provided that the anti configuration can be retained during the whole reaction process. In fact, the energetically favorable nonadiabatic pathway is shown to possess the downward potential energy profile and low barriers, indicating that the SP photoreaction should proceed rapidly, and thus the two thymine residues do not have time to change their relative positions and steric conformations. This explains why the initial anti configuration of TpT can be retained during the whole reaction process and only the SP product with 5R steric configuration is yielded from the reaction.

We have also explored the possibility for a concerted mechanism which should involve a simultaneous hydrogen atom transfer and a cross-link of the allylic C7′ to C5 between the two thymine residues in TpT. In the triplet state, simply no

concerted transition state could be located. In the singlet ground state, a concerted transition state STSC with a barrier of 70.4 kcal mol^{-1} is located, as shown in Figure 2b. But intrinsic reaction coordinate calculations show that this transition state leads to the C5–C6′ cross-linked product (denoted as P2 in Figure 1), instead of forming a C5–C7′ bond as in the SP reaction. As shown with the optimized structures in Figure 1, the concerted reaction product P2 is obviously not the SP product. Closely examining the concerted transition structure STSC, we find that the C5...C7′ distance (3.34 Å) is 0.25 Å longer than the C5...C6′ distance (3.09 Å), which is the reason why the C5–C6′ cross-link product is yielded, but not the SP product. Therefore, the concerted mechanism can be ruled out toward the SP formation. On the other hand, the concerted path toward the C5–C6′ cross-link product is obviously unlikely to occur because of its large endothermicity of 31.4 kcal mol^{-1} and high barrier of 70.4 kcal mol^{-1}, as shown in Table 1 and Figure 2b.

4. CONCLUSION

In the present work, we have explored the photochemical reaction pathways of TpT dinucleotides toward the formation of a DNA photolesion product, spore photoproduct (SP). The potential energy profiles for the SP formation in the possible lowest-lying triplet and singlet ground state as well as the interaction between these two states were calculated at the B3LYP/6-311++G(d, p)//B3LYP/6-311G(d, p) level of theory. The reaction pathways on the singlet excited state S_1 were also explored on the basis of TD-DFT calculations using the S_0 stationary structures.

Our calculations show that the reaction follows consecutive mechanisms along either of S_1, T_1, or S_0 states, which involves the initial hydrogen atom transfer from the 3′-T methyl to C6 of 5′-T and a subsequent C5–CH$_2$ bond formation linking 3′-T and 5′-T. However, all the adiabatic reaction pathways proceeding though S_1, T_1, or S_0 states alone are shown to be energetically infeasible, while the nonadiabatic pathway involving both T_1 and S_0 states corresponds to the lowest energy path and is the most favorable in energy. Such a nonadiabatic pathway involves an initial hydrogen atom transfer with a barrier of 14.2 kcal mol^{-1} (11.9 kcal mol^{-1} in bulk solution) along the T_1 state forming the triplet biradical intermediate TI, from which the T_1/S_0 surface crossing occurs and the subsequent C5–CH$_2$ bond formation toward the final SP formation proceeds facilely in the S_0 state after intersystem crossing from the triplet biradical TI to the singlet biradical SI, with a barrier of only 5.9 kcal mol^{-1} (3.8 kcal mol^{-1} in bulk solution). Thus, the whole reaction along such a nonadiabatic pathway is rate-limited by the hydrogen atom transfer from the 3′-T methyl group to the C6 of the 5′-T residue. This result provides a rationale for the experimentally observed kinetic isotope effect of 3.5 after deuterium substitution at the 3′-T methyl group of TpT.[12]

AUTHOR INFORMATION

Corresponding Author
*E-mail: hongmei@iccas.ac.cn.

Author Contributions
†These authors contributed equally.

Notes
The authors declare no competing financial interest.

REFERENCES

(1) Matsumura, Y.; Ananthaswamy, H. N. *Toxicol. Appl. Pharmacol.* **2004**, *195* (3), 298–308.
(2) Slieman, T. A.; Rebeil, R.; Nicholson, W. L. *J. Bacteriol.* **2000**, *182* (22), 6412–6417.
(3) Desnous, C.; Guillaume, D.; Clivio, P. *Chem. Rev.* **2010**, *110* (3), 1213–1232.
(4) Guo, J. D.; Luo, Y.; Himo, F. *J. Phys. Chem. B* **2003**, *107* (40), 11188–11192.
(5) Yang, L. L.; Lin, G. J.; Liu, D. G.; Dria, K. J.; Telser, J.; Li, L. *J. Am. Chem. Soc.* **2011**, *133* (27), 10434–10447.
(6) Benjdia, A.; Heil, K.; Barends, T. R. M; Carell, T; Schlichting, I. *Nucleic Acids Res.* **2012**, DOI: 10.1093/nar/gks603.
(7) Donnella.Je; Setlow, R. B. *Science* **1965**, *149* (3681), 308–309.
(8) Mantel, C.; Chandor, A.; Gasparutto, D.; Douki, T.; Atta, M.; Fontecave, M.; Bayle, P. A.; Mouesca, J. M.; Bardet, M. *J. Am. Chem. Soc.* **2008**, *130* (50), 16978–16984.
(9) Cadet, J.; Vigny, P. *The Photochemistry of Nucleic Acids*; John Wiley: New York, 1990.
(10) Wang, S. Y. *Photochemistry and Photobiology of Nucleic Acids*; Academic Press: New York, 1976.
(11) Varghese, A. J. *Biochem. Biophys. Res. Commun.* **1970**, *38* (3), 484–490.
(12) Lin, G. J.; Li, L. *Angew. Chem., Int. Ed.* **2010**, *49* (51), 9926–9929.
(13) Kim, S. J.; Lester, C.; Begley, T. P. *J. Org. Chem.* **1995**, *60* (20), 6256–6257.
(14) Lin, G. J.; Chen, C. H.; Pink, M.; Pu, J. Z.; Li, L. *Chem.—Eur. J.* **2011**, *17* (35), 9658–9668.
(15) Heil, K.; Kneuttinger, A. C.; Schneider, S.; Lischke, U.; Carell, T. *Chem.—Eur. J.* **2011**, *17* (35), 9651–9657.
(16) Chandra, T.; Silver, S. C.; Zilinskas, E.; Shepard, E. M.; Broderick, W. E.; Broderick, J. B. *J. Am. Chem. Soc.* **2009**, *131* (7), 2420–2421.
(17) Zhang, R. B.; Eriksson, L. A. *J. Phys. Chem. B* **2006**, *110* (14), 7556–7562.
(18) Yang, Z. B.; Zhang, R. B.; Eriksson, L. A. *Phys. Chem. Chem. Phys.* **2011**, *13* (19), 8961–8966.
(19) Hare, P. M.; Crespo-Hernandez, C. E.; Kohler, B. *Proc. Natl. Acad. Sci. U.S.A.* **2007**, *104* (2), 435–440.
(20) Yang, C.; Yu, Y.; Liu, K.; Song, D.; Wu, L.; Su, H. *J. Phys. Chem. A* **2011**, *115* (21), 5335–5345.
(21) Frisch, M. J.; et al. *Gaussian 03*, revision B.03; Gaussian, Inc.: Wallingford, CT, 2004.
(22) Becke, A. D. *J. Chem. Phys.* **1993**, *98* (7), 5648–5652.
(23) Lee, C. T.; Yang, W. T.; Parr, R. G. *Phys. Rev. B* **1988**, *37* (2), 785–789.
(24) Gonzalez, C.; Schlegel, H. B. *J. Phys. Chem.* **1990**, *94* (14), 5523–5527.
(25) Mennucci, B.; Tomasi, J. *J. Chem. Phys.* **1997**, *106* (12), 5151–5158.
(26) Stratmann, R. E.; Scuseria, G. E.; Frisch, M. J. *J. Chem. Phys.* **1998**, *109* (19), 8218–8224.
(27) Vanderlu, W. T.; Oosterho, L. J. *J. Am. Chem. Soc.* **1969**, *91* (22), 6042–6049.
(28) Durbeej, B.; Eriksson, L. A. *J. Photochem. Photobiol., A* **2002**, *152* (1–3), 95–101.
(29) Borden, W. T.; Davidson, E. R. *J. Am. Chem. Soc.* **1977**, *99* (14), 4587–4594.
(30) Havenith, R. W. A.; van Lenthe, J. H.; Jenneskens, L. W. *J. Org. Chem.* **2005**, *70* (11), 4484–4489.